Research Square

Preprints are preliminary reports that have not undergone peer review.
They should not be considered conclusive, used to inform clinical practice,
or referenced by the media as validated information.

Extracellular Volume Fraction Derived from Contrast-Enhanced CT for Predicting Occult Lymph Node Metastasis in Colorectal Cancer

Jing Ma

missingshz@163.com

Xinjiang production and Construction Corps Hospital

Zehua Wang

Xinjiang production and Construction Corps Hospital

Zhiqiang Song

Xinjiang production and Construction Corps Hospital

Dong Wang

Shihezi People's Hospital

Xihui Chen

The Sixth Division Hospital of Xinjiang Production and Construction Corps

Ying Wu

Xinjiang production and Construction Corps Hospital

Zhipeng Huang

Xinjiang production and Construction Corps Hospital

Research Article

Keywords: Colorectal cancer, Occult lymph node metastasis, Extracellular volume fraction, Contrast-enhanced CT, Nomogram

Posted Date: August 31st, 2026

DOI: https://doi.org/10.21203/rs.3.rs-10327620/v1

License: This work is licensed under a Creative Commons Attribution 4.0 International License.
Read Full License

Additional Declarations: No competing interests reported.

Extracellular Volume Fraction Derived from Contrast-Enhanced CT for Predicting Occult Lymph Node Metastasis in Colorectal Cancer

Abstract

Objective To investigate the predictive value of contrast-enhanced CT delayed-phase extracellular volume fraction (fECV) for occult lymph node metastasis (OLNM) in colorectal cancer (CRC) and to develop a combined prediction model.

Methods A total of 182 surgically confirmed CRC patients were retrospectively enrolled. OLNM was defined as negative preoperative CT findings but positive postoperative pathology. Patients were randomly split into training (n=127) and test (n=55) cohorts (7:3). fECV was calculated from preoperative CT. Univariate and multivariate logistic regression identified independent predictors, followed by construction of an fECV-only model and a combined nomogram. Model performance was assessed using ROC curves, calibration curves, and decision curve analysis.

Results The OLNM group showed significantly higher fECV than the non-OLNM group in the training set (37.95 vs. 29.93, P<0.001). Multivariate regression identified lymph node aggregation (LNA; OR=5.566, 95%CI: 1.794–17.267, P=0.003) and fECV (OR=1.077, 95%CI: 1.021–1.137, P=0.006) as independent predictors. The fECV-only model achieved AUCs of 0.801 (training) and 0.800 (test).

The nomogram integrating LNA and fECV achieved superior discrimination, with AUCs of 0.847 and 0.897, respectively (both $P<0.05$). Calibration curves demonstrated good consistency, and decision curve analysis confirmed greater clinical net benefit of the nomogram.

Conclusion CT delayed-phase fECV is a reliable quantitative imaging biomarker for OLNM in CRC. The LNA-fECV nomogram enables accurate, noninvasive preoperative prediction, supporting personalized risk stratification and clinical decision-making.

Keywords: Colorectal cancer; Occult lymph node metastasis; Extracellular volume fraction; Contrast-enhanced CT; Nomogram

Introduction

Colorectal cancer is among the most common malignancies worldwide and has high incidence and mortality rates [1-3]. Lymph node metastasis (LNM) is a key factor affecting postoperative recurrence, long-term survival and adjuvant treatment strategies in CRC patients [4]. In clinical practice, a special phenomenon is frequently observed: some patients have no obviously enlarged lymph nodes on preoperative CT (short-axis diameter < 10 mm with regular morphology), whereas postoperative pathological examination confirms lymph node metastasis, namely, occult lymph node metastasis (OLNM). The presence of OLNM leads to an underestimation of clinical stage, thereby causing delayed or omitted adjuvant chemotherapy and seriously impairing patient prognosis [5].

At present, CT remains the most commonly used imaging modality for the preoperative staging of CRC [6]. However, its evaluation of LNM relies mainly on morphological features such as lymph node size and shape, resulting in a low sensitivity of 30–50% for detecting OLNM [7,8]. In recent years, radiomics and machine learning have shown certain potential, but unified quantitative criteria are still lacking, and their generalizability requires further verification [9-11].

Remodeling of the extracellular matrix (ECM) is a core biological process of tumor invasion and metastasis [12-13]. The extracellular volume fraction (fECV) calculated from the equilibrium phase of contrast-enhanced CT can quantitatively reflect the volume proportion of ECM in tissues. Previous studies have proven that fECV can effectively predict pathological grade, microvascular invasion and postoperative survival in patients with various types of cancer, including liver cancer and pancreatic cancer [14-16]. In CRC patients, an elevated fECV has been preliminarily correlated with the development of adverse pathological features such as perineural invasion and vascular invasion [17-18]. Nevertheless, its value in predicting OLNM has not been systematically reported.

Accordingly, this study aimed to investigate the predictive efficacy of fECV derived from the delayed phase of contrast-enhanced CT to predict OLNM in CRC patients. An intuitive nomogram was constructed by

integrating valuable imaging features to provide evidence for accurate preoperative identification of patients at high risk of OLNM.

1 Materials and Methods

1.1 Study Population

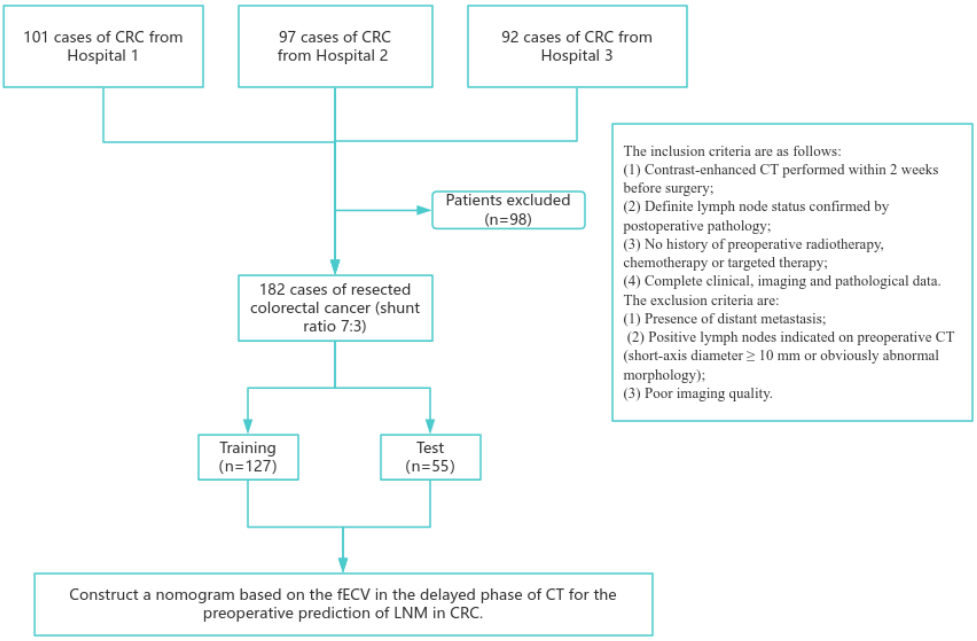
This multicenter retrospective study was approved by the institutional ethics committee. A total of 212 patients who were diagnosed with CRC via postoperative pathology testing between January 2020 and July 2025 were initially enrolled, and 182 eligible patients were ultimately included.

Inclusion criteria: (1) Contrast-enhanced CT performed within 2 weeks before surgery; (2) Definite lymph node status confirmed by postoperative pathology; (3) No history of preoperative radiotherapy, chemotherapy or targeted therapy; (4) Complete clinical, imaging and pathological data.

Exclusion criteria: (1) Presence of distant metastasis; (2) Positive lymph nodes indicated on preoperative CT (short-axis diameter ≥ 10 mm or obviously abnormal morphology); (3) Poor imaging quality.

All the subjects were randomly divided into a training group (127 patients) and a test group (55 patients) at a ratio of 7:3 (see Figures 2).

Figure 1 Flow chart of patient selection in the study.



1.2 Definition of Occult Lymph Node Metastasis

OLNM was defined as the presence of negative lymph nodes on preoperative CT assessment (all regional lymph nodes with short-axis diameter < 10 mm and regular morphology), while tumor cell metastasis was detected in at least one lymph node on postoperative pathological examination.

1.3 Preoperative Clinical and Histopathological Data

Baseline data, including sex, age and routine blood parameters such as hematocrit (HCT) level, platelet (PLT) count, lymphocyte (LN) count and neutrophil (NE) count, were collected from clinical records. The tumor biomarkers included carcinoembryonic antigen (CEA) and carbohydrate antigen 19-9 (CA19-9). Pathological data were obtained from the central pathology departments of the participating hospitals.

1.4 CT Examination Protocol

All scans were performed mainly using a 320-slice spiral CT scanner. Patients received breathing training before scanning, with the scanning range extending from the diaphragm to the inferior margin of the pubic symphysis. Scan parameters were set as follows: tube voltage, 120 kV; automatic tube current modulation (reference tube current, 130 mAs); gantry rotation time, 0.5 s; and pitch, 0.9937. A high-concentration nonionic contrast agent, iomeprol (iodine content: 350 mgI/mL), was injected via the antecubital vein with a high-pressure syringe at a flow rate of 4 mL/s and a total dose of 0.8–1.2 mL/kg. After contrast agent injection, 20 mL of normal saline was injected at the same flow rate. Images were acquired using the threshold monitoring method with a threshold of 200 HU. Arterial phase scanning started 8 seconds after the threshold was reached; the venous phase was 27 seconds, and the delayed phase was 200 seconds.

1.5 Image Measurement Methods

Raw CT data were reconstructed with a slice thickness of 5 mm using the ULInnovation-CT platform (R001; United Imaging Healthcare, Shanghai, China). CT values of lesions and large arteries (aorta or iliac artery) on unenhanced and delayed phase images were measured. The region of interest (ROI) was placed on the enhanced marginal area of the lesion on the arterial phase image, with an area of 30–60 mm^2. Hemorrhage, cystic degeneration, calcification and blood vessels were avoided as much as

possible. ROIs were delineated on the maximum lesion slice and two adjacent slices, and corresponding arterial ROIs on the same slices were also measured. The arterial ROI was drawn as large as possible to reduce measurement errors. Each ROI was measured three times and the average value was calculated. The fECV of the lesion was calculated using the following formula: $fECV(\%)=(1-HCT)\times(\Delta HUROI/\Delta HUartery)\times100\%$. Hematocrit (HCT) levels were determined from routine blood tests within one week before CT examination. ΔHUROI refers to the difference in CT values of the lesion ROI between the delayed phase and unenhanced phase. ΔHUartery represents the difference in CT values of the arterial ROI between the delayed phase and unenhanced phase (see Supplementary Figures 1 and 2). In addition, the maximum short-axis diameter of the lymph nodes and the maximum longitudinal diameter of the intestinal wall involving the lesion were also measured.

1.6 Evaluation of Imaging Features

Two abdominal radiologists (with 7 and 9 years of working experience) independently evaluated the following imaging features in a blinded manner but did not know the pathological results:

Multiple lymph node metastasis (MLNM): ≥ 2 lymph nodes with a short-axis diameter ≥ 5 mm.

Maximum short-axis diameter of the lymph node (MSDLN): The maximum short-axis diameter (mm) of regional lymph nodes.

□Lymph node aggregation (LNA): ≥ 3 adjacent lymph nodes on the same image slice.

□Lymph node fusion (LNF): Blurred or disappeared boundaries between adjacent lymph nodes.

□Lymph node distribution along arteries (LNDA): Lymph nodes distributed along the arterial course.

□Blurred lesion margin (BLM): Obscured fat space between the primary tumor and surrounding tissues.

□Maximum lesion length (MLL): The maximum longitudinal diameter (cm) of the primary tumor.

1.7 Construction and test of the Clinical Model, fECV Model and Nomogram

Univariate and multivariate logistic regression analyses were performed to screen independent risk factors for LNM in CRC patients. A clinical model was constructed on the basis of clinical risk factors, and an fECV model was established using the fECV alone. A nomogram combining clinical risk factors and fECV was developed to predict LNM. Model performance was assessed by the area under the ROC curve (AUC), accuracy, sensitivity, specificity, positive predictive value (PPV) and negative predictive value (NPV). The Hosmer–Lemeshow test and calibration curves were used to evaluate the calibration of the nomogram. Decision curve analysis (DCA) was applied to assess the clinical utility of

the nomogram for LNM prediction.

1.8 Statistical Analysis

Data analysis was performed using SPSS 27.0 and R 4.1.1 software. Normally distributed continuous variables are expressed as mean ± standard deviation and were compared using the independent-samples t test. Nonnormally distributed continuous variables are presented as median (interquartile range) and were compared using the Mann–Whitney U test. Categorical variables are described as percentages and were compared using the chi-square test or Fisher's exact test. Interobserver agreement between the two radiologists was assessed by the intraclass correlation coefficient (ICC); an ICC > 0.75 indicated good agreement. A P value < 0.05 was considered to indicate statistical significance.

Results

1 Baseline Characteristics

Good interobserver reproducibility was observed for all measurements and imaging assessments (all ICCs > 0.75). As shown in Table 1, there were no significant differences in age, sex, routine blood parameters, tumor biomarkers, imaging features and fECV values between the training dataset and test dataset (all P > 0.05), suggesting good comparability between the two groups.

Table 1 Baseline characteristics of patients in the training set and validation set.

Variable	Total cohort (n=182)	Training cohort (n=127)	Validation cohort (n=55)
LNM	64 (35.2)	45 (35.4)	19 (34.5)
Age (years)	69 (59, 77)	70 (61, 78)	66.98±10.45
Male	86(47.3)	62(48.8)	24 (43.6)
HCT (%)	37.7 (31.98, 41.33)	37.5 (31.8, 41.1)	38.3 (34.1, 41.9)
PLT(10^9/L)	234.5 (191.75, 308.5)	237 (192, 314)	233 (191, 271)
LN(10^9/L)	2.01 (1.42, 17.53)	2.01(1.35, 22.6)	2.12(1.64, 10)
NE(10^9/L)	5.26 (3.45, 55.58)	5.77 (3.66, 58.6)	4.66 (3.09, 53.2)
CEA(ng/mL)	4.12 (2.17, 12.92)	4.5 (2.32, 13.64)	3.41(1.94, 12.77)
CA19-9 (U/mL)	10.60 (4.97, 20.28)	10.86 (5, 22.08)	10.16 (4.32, 16.99)
MLNM	68 (37.4)	47 (37)	21 (38.2)
MSDLN (mm)	5.3 (4, 7)	5.3 (4, 7.1)	5.45±2
LNA	92 (50.5)	66 (52)	26 (47.3)
LNF	33 (18.1)	24 (18.9)	9 (16.4)
LNDA	174 (95.6)	121 (95.3)	53 (96.4)
BLM	130 (71.4)	95(74.8)	35 (63.6)
MLL (cm)	4.5 (3.2, 6.025)	4.5（3.1，6）	4.6 (4, 6.4)
fECV	33.1 (28.03, 39.1)	32.5 (28.84, 39.8)	33.04 (28.84, 47.87)

Abbreviations: LNM, lymph node metastasis; HCT, hematocrit; PLT, platelet count; LN, lymphocyte count; NE, neutrophil count; CEA, carcinoembryonic antigen; CA19-9, carbohydrate antigen 19-9; MLNM, multiple lymph node metastases; MSDLN, maximum short diameter of lymph nodes; LNA, lymph node aggregation; LNF, lymph node fusion; LNDA, lymph node distribution along the artery; BLM, blurred lesion margin; MLL, maximum length of the lesion; fECV, extracellular volume fraction

2 Univariate Analysis

In the training dataset, univariate analysis revealed significant differences in MSDLN, LNA, LNF, BLM and fECV between the OLNM group and the non-OLNM group (all $P < 0.05$). Notably, the fECV was markedly greater in the OLNM group (37.95 vs. 29.93, $P < 0.001$) (Table 2).

Table 2 Univariable logistic regression analysis results.

Variable	non-LNM (n=82)	LNM (n=45)	X^2/t/Z	OR (95% CI)	P value
Age (years)	69.65±11.16	67.29±11.24	-1.136	0.981(0.950~1.014)	0.258
Male	41(50)	21 (46.7)	0.129	0.875(0.422~1.813)	0.719
HCT (%)	37.7 (31.9, 40.85)	36.9（30,41.5）	-0.736	0.978(0.928~1.030)	0.462
Plt(10^9/L)	242.4±80.37	273（194，342.5）	-1.779	1.005 (1~1.009)	0.075
LN(10^9/L)	2.15 (1.47, 24.1)	1.43 (1.17, 11.05)	-2.19	0.982 (0.954~1.011)	0.029
NE(10^9/L)	6.5 (4.11, 61.8)	4.65 (3.22, 46)	-1.883	0.989 (0.977~1.002)	0.06
CEA(ng/mL)	3.93（2.15，9.65）	5.43（2.34,17.76）	-1.51	1.004（0.997~1.010）	0.131
CA199 (U/mL)	10.99（4.84，21.15）	10.75 (5.18, 24.43)	-0.136	1.006(0.998~1.013)	0.892
MLNM	25 (30.5,)	22 (48.9)	4.22	2.181(1.030~4.617)	0.040
MSDLN (mm)	4.5 (3.5, 6.35)	6.3 (4.95, 8.1)	-4.091	1.541(1.240~1.916)	0.001
LNA	29 (35.4)	37 (82.2)	25.56	8.453(3.477~20.547)	0.001
LNF	11 (13.4)	13 (28.9)	4.54	2.622(1.061~6.481)	0.033
LNDA	78 (95.1)	43 (95.6)	0.012	1.103(0.194~6.267)	0.912
BLM	53 (64.6)	43(93.3)	12.7	7.660(2.182~26.891)	0.001
MLL (cm)	4.79±1.89	4.66±1.91	-0.386	0.962(0.792~1.168)	0.7
fECV	29.93 (26.11, 34.56)	37.95 (33.81, 44.15)	-5.59	1.110(1.055~1.169)	0.001

Abbreviations: non-LNM: non-lymph node metastasis; LNM: lymph node metastasis; OR, odds ratio; CI, confidence interval

3 Multivariate Analysis

Variables with statistical significance in univariate analysis were included in the multivariate logistic regression model. The results (Table 3) revealed that lymph node aggregation (LNA) (OR = 5.566; 95% CI: 1.794–17.267; P = 0.003) and fECV (OR = 1.077; 95% CI: 1.021–1.137; P = 0.006) were independent risk factors for OLNM in CRC patients. MLNM, MSDLN, LNF and BLM were not retained in the final model.

Table 3 Multivariable Logistic Regression Analysis

Variable	βvalue	Standard error	Wald value	P value	OR	95%Cl
LN(10^9/L)	−0. 012	0. 018	0. 44	0. 507	0. 988	0. 953~1. 024
MLNM	−0. 588	0. 629	0. 875	0. 35	0. 555	0. 162~1. 905
MSDLN (mm)	0. 18	0. 192	0. 882	0. 348	1. 197	0. 822~1. 744
LNA	1. 717	0. 578	8. 832	0. 003	5. 566	1. 794~17. 267
LNF	−0. 207	0. 584	0. 126	0. 723	0. 813	0. 259~2. 553
BLM	1. 081	0. 734	2. 166	0. 141	2. 947	0. 699~12. 434
fECV	0. 074	0. 027	7. 442	0. 006	1. 077	1. 021~1. 137

4 Predictive Performance of the Models

A nomogram was constructed by integrating fECV and LNA (Figure 2). As presented in Table 4 and Figure 3, the AUC values of the single fECV model for OLNM prediction were 0.801 (95% CI: 0.724–0.877) in the training dataset and 0.800 (95% CI: 0.668–0.931) in the test dataset. The nomogram combining LNA and fECV achieved better performance, with AUC values increasing to 0.847 (95% CI: 0.777–0.916) and 0.897 (95% CI: 0.817–0.977), respectively. No significant difference was found between the models according to the DeLong test (all $P > 0.05$).

Figure 2 Nomogram for predicting lymph node metastasis status in the training set

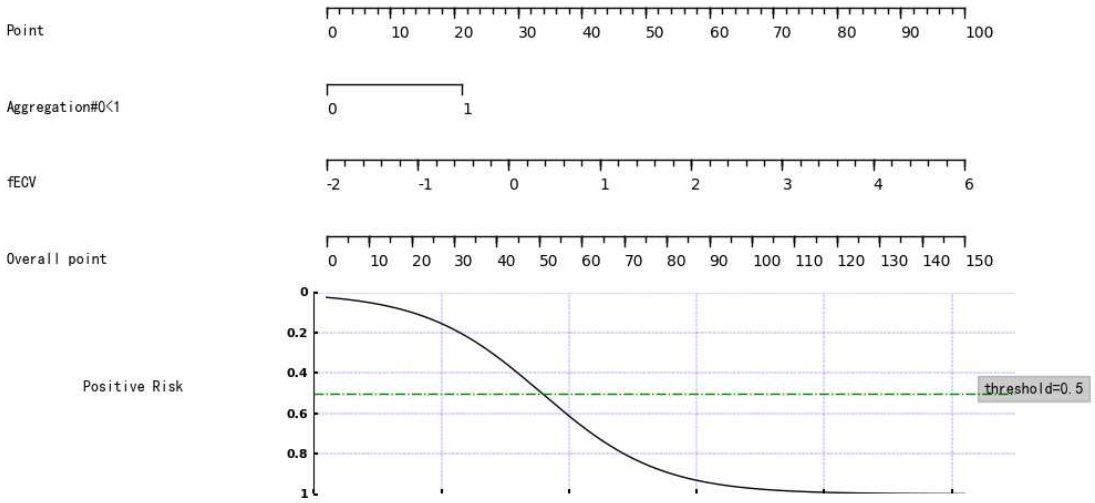
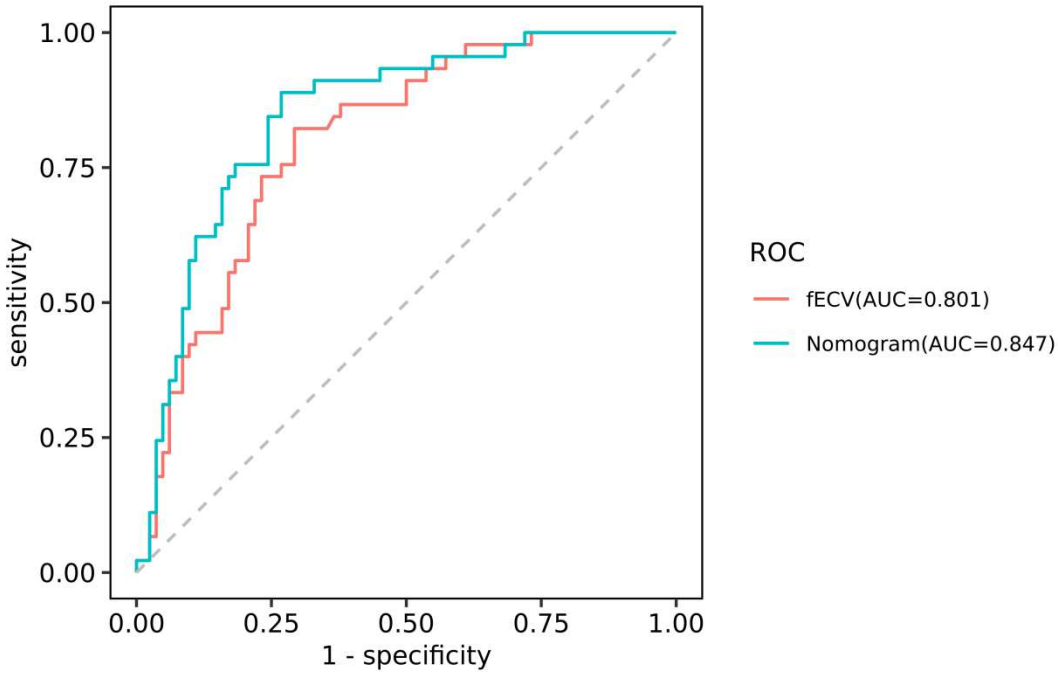


Table 4 Performance of the models for predicting lymph node status in patients with colorectal cancer.

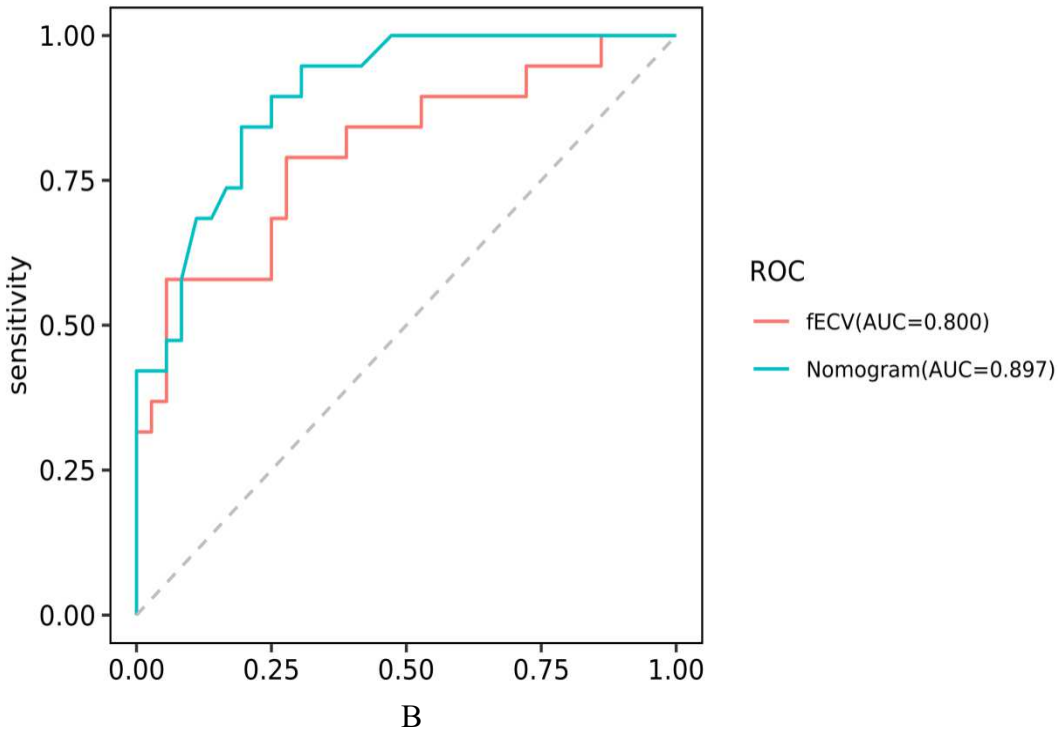
		AUC (95% CI)	OCV	Se	Sp	Max J
fECV	Training	0.801（0.724-0.877 ）	33.365	0.822	0.707	0.53
	Test	0.8 （0.668-0.931 ）	48.12	0.579	0.944	0.523
Nomogram	Training	0.847（0.777-0.916 ）	0.345	0.889	0.732	0.621
	Test	0.897（0.817-0.977 ）	0.355	0.842	0.806	0.648

Abbreviations: AUC, area under the receiver operating characteristic curve; OCV, optimal Cut-off Value; Se, sensitivity; Sp, specificity; Max J, youden's Index

Figure 3 Receiver operating characteristic curves of the fECV and nomogram models for prediction in the training set (A) and validation set (B).



A



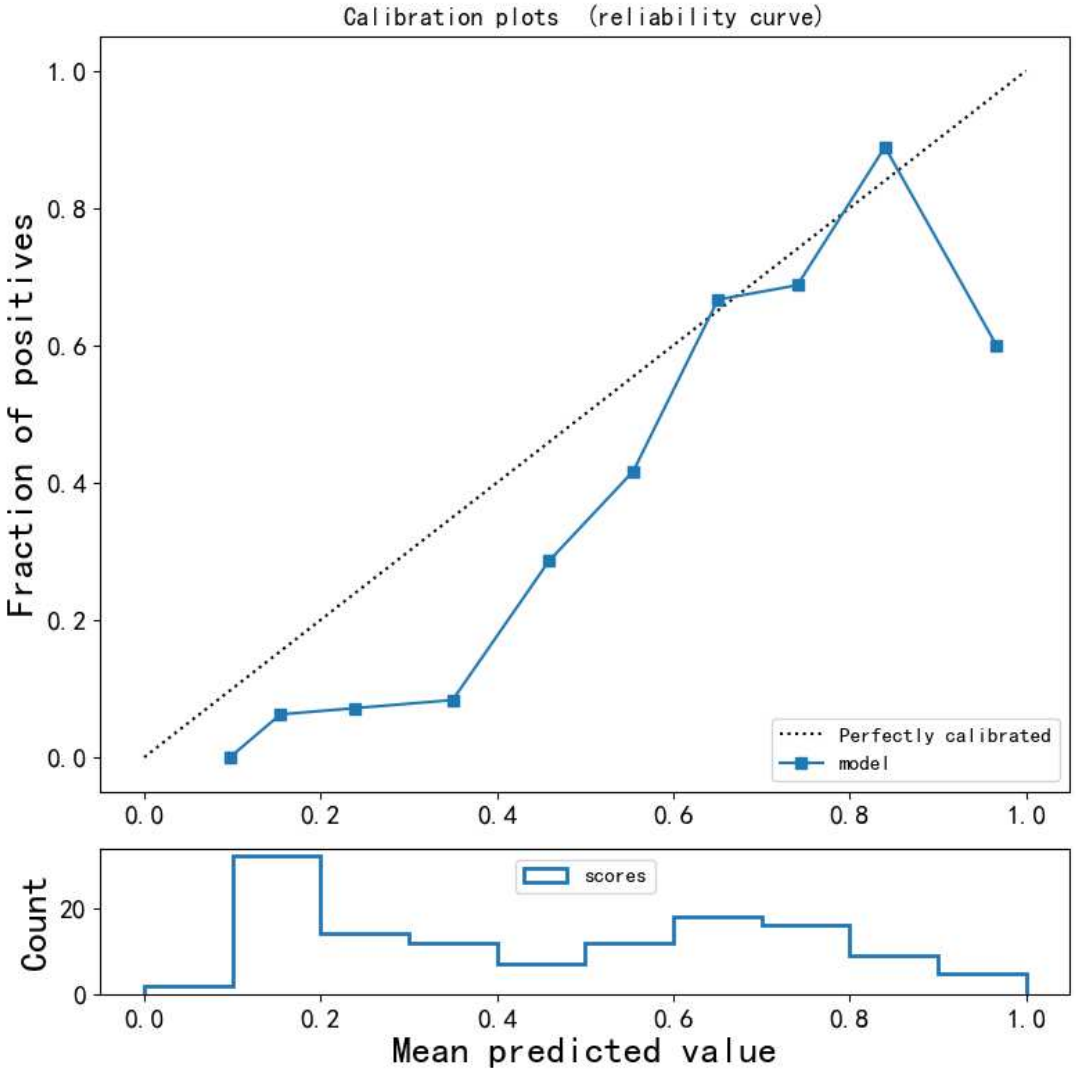
B

5 Model Calibration and Clinical Utility

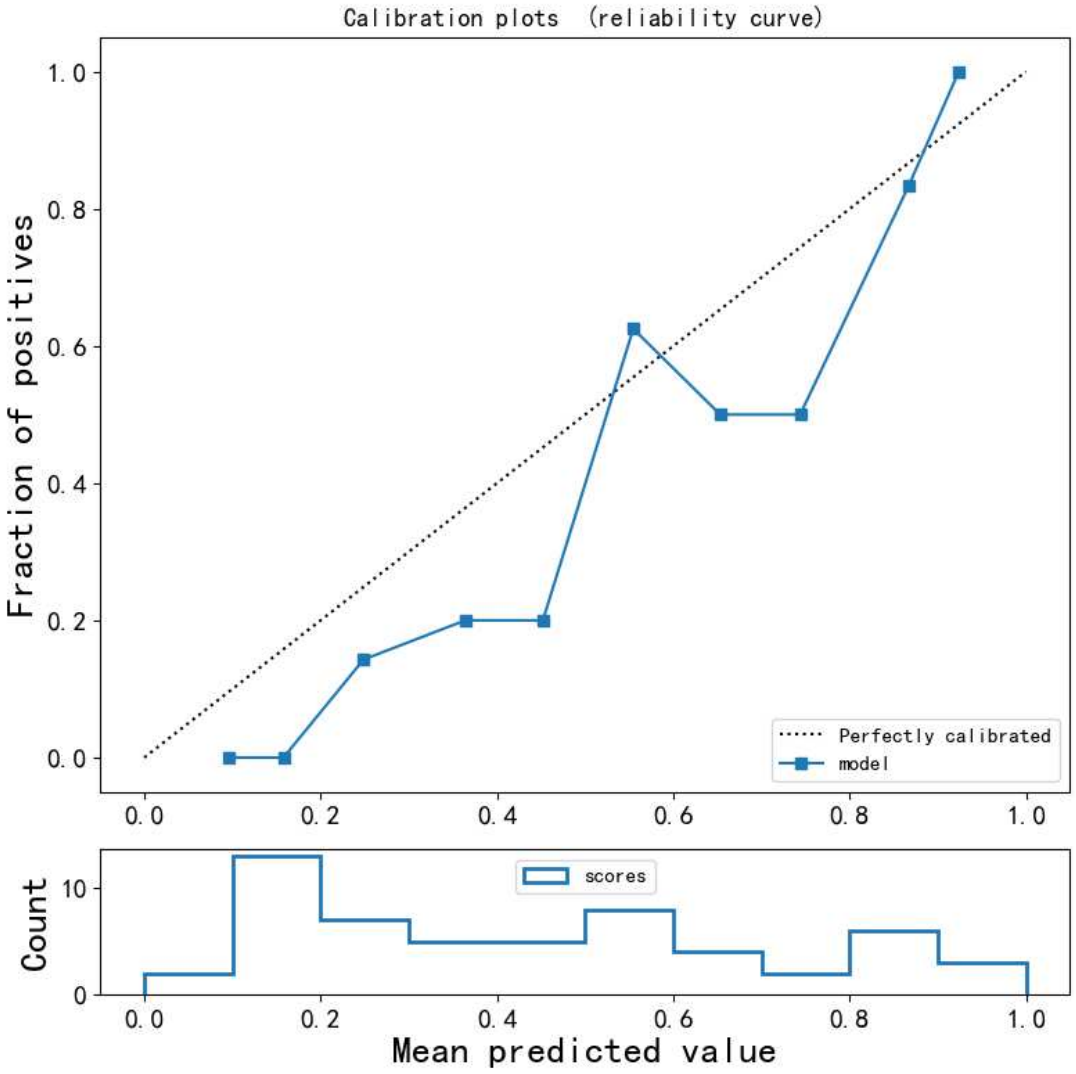
Calibration curves (Figure 4A, 4B) demonstrated good consistency between the predicted OLNM probability and actual outcomes (Hosmer–

Lemeshow test, all P > 0.05). Decision curve analysis (Figure 5) indicated that the combined nomogram provided greater clinical net benefit than the single fECV model across a wide range of risk thresholds.

Figure 4 Calibration curves in the training set (A) and validation set (B).

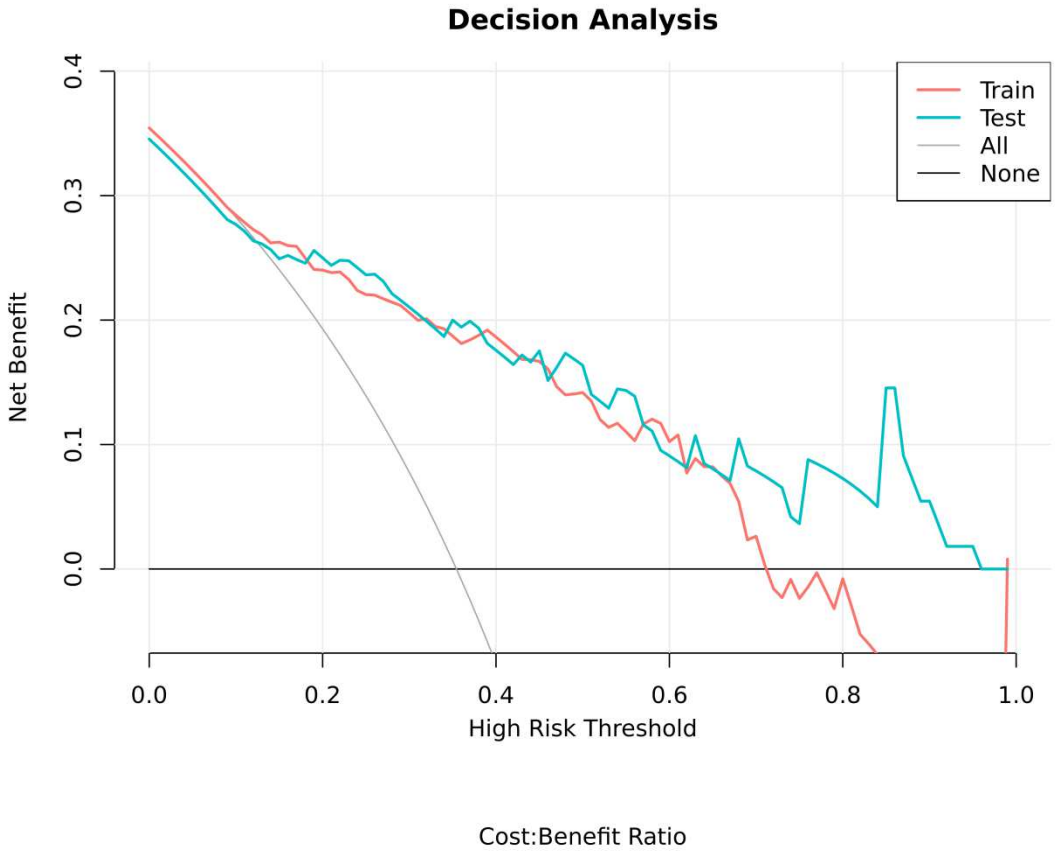


A



B

Figure 5 Decision curve analysis of the nomogram.



Discussion

OLNM is a blind spot in the preoperative staging of colorectal cancer, and its accurate identification is critical for formulating individualized treatment regimens. To our knowledge, this is the first study to systematically explore the predictive value of fECV derived from delayed-phase contrast-enhanced CT for OLNM in CRC. We successfully constructed a nomogram integrating fECV and the imaging feature LNA. The results confirmed that both fECV and LNA were independent predictors of OLNM, and the combined nomogram clearly improved the predictive performance, providing a noninvasive and quantitative tool for preoperative clinical evaluation.

This study verified that primary tumors of OLNM patients had higher fECV values. Elevated fECV pathologically reflects abnormal ECM remodeling in the tumor microenvironment [11-12]. Activated cancer-associated fibroblasts (CAFs) secrete large quantities of ECM components such as collagen, accompanied by increased vascular permeability, which leads to the expansion of the extracellular space [19-20]. This tumor-invasive microenvironment not only promotes local progression of primary lesions but also remodels lymphangiogenesis and lymphatic drainage pathways, creating conditions for occult dissemination of tumor cells to regional lymph nodes [21-22]. These findings are consistent with those of previous studies by Cheng et al. [17] and Zheng et al. [18] on CRC, further supporting the use of the fECV as a quantitative imaging biomarker reflecting the overall invasive potential of tumors.

LNA, defined as the aggregation of multiple small lymph nodes, was identified as another independent predictor. Even if the short-axis diameter of these lymph nodes does not reach the traditional positive threshold (< 10 mm), their aggregated pattern may represent an early nonspecific reaction of regional lymph nodes to tumor metastasis (e.g., medullary hyperplasia or paracortical enlargement) or indicate tumor invasion at multiple sites along lymphatic drainage routes [23]. Guan et al. [23] also emphasized the value of lymph node distribution patterns in

predicting LNM. Our findings extend this conclusion to patients with OLNM and highlight the complementary role of morphological features to functional imaging.

Notably, traditional morphological indicators, including MSDLN and LNF, were not independent predictors in the OLNM cohort. This reveals the essential feature of occult metastasis: lymph nodes present no obvious morphological changes at this stage. Reliance merely on lymph node size or destructive changes such as fusion inevitably leads to missed diagnoses. Therefore, combining fECV (which reflects microenvironmental changes) and LNA (which indicates early abnormal spatial distribution of lymph nodes) can sensitively capture subtle signs of OLNM.

Several limitations of this study should be acknowledged. First, owing to its retrospective nature and limited sample size, this study may have selection bias; additionally, precise matching between pathological and selected imaging images could not be guaranteed. To mitigate these limitations, future investigations should enroll a larger prospective cohort and strictly conduct one-to-one matching of pathological specimens and imaging data. Second, fECV was measured based on manually delineated two-dimensional ROIs, which failed to reflect intratumoral heterogeneity. Machine learning based on whole-tumor segmentation will be adopted in future research. Third, subgroup analysis between patients with colon cancer and those with rectal cancer was not performed. Given the

differences in biological behavior and lymph node metastasis patterns between the two diseases, a stratified analysis will be conducted in subsequent studies.

Conclusion

The extracellular volume fraction calculated from the delayed phase of contrast-enhanced CT is an effective quantitative imaging biomarker for predicting occult lymph node metastasis in patients with colorectal cancer. The nomogram combined with lymph node aggregation achieves high-precision and noninvasive prediction of OLNM and provides an important reference for preoperative individualized risk assessment and adjuvant treatment decision-making.

References

[1]Ferlay J, Soerjomataram I, Dikshit R, Eser S, Mathers C, Rebelo M, Parkin DM, Forman D, Bray F. Cancer incidence and mortality worldwide: sources, methods and major patterns in GLOBOCAN 2012. Int J Cancer. 2015 Mar 1;136(5):E359-86. doi: 10.1002/ijc.29210.

[2]Bray F, Ferlay J, Soerjomataram I, Siegel RL, Torre LA, Jemal A. Global cancer statistics 2018: GLOBOCAN estimates of incidence and mortality worldwide for 36 cancers in 185 countries. CA Cancer J Clin. 2018 Nov;68(6):394-424. doi: 10.3322/caac.21492. Epub

2018 Sep 12. Erratum in: CA Cancer J Clin. 2020 Jul;70(4):313. doi: 10.3322/caac.21609.

[3]Bray F, Laversanne M, Sung H, Ferlay J, Siegel RL, Soerjomataram I, Jemal A. Global cancer statistics 2022: GLOBOCAN estimates of incidence and mortality worldwide for 36 cancers in 185 countries. CA Cancer J Clin. 2024 May-Jun;74(3):229-263. doi: 10.3322/caac.21834. Epub 2024 Apr 4.

[4]Huh JW, Jeong YY, Kim HR, Kim YJ. Prognostic value of preoperative radiological staging assessed by computed tomography in patients with nonmetastatic colon cancer. Ann Oncol. 2012 May;23(5):1198-1206. doi: 10.1093/annonc/mdr404. Epub 2011 Sep 23.

[5]Nerad E, Lahaye MJ, Maas M, Nelemans P, Bakers FC, Beets GL, Beets-Tan RG. Diagnostic Accuracy of CT for Local Staging of Colon Cancer: A Systematic Review and Meta-Analysis. AJR Am J Roentgenol. 2016 Nov;207(5):984-995. doi: 10.2214/AJR.15.15785.

[6]Bai RJ, Ren SH, Jiang HJ, Li JP, Liu XC, Xue LM. Accuracy of Multi-Slice Spiral Computed Tomography for Preoperative Tumor Node Metastasis (TNM) Staging of Colorectal Carcinoma. Med Sci Monit. 2017 Jul 17;23:3470-3479. doi: 10.12659/msm.902649.

[7]Abbaspour E, Karimzadhagh S, Monsef A, Joukar F, Mansour-Ghanaei F, Hassanipour S. Application of radiomics for

preoperative prediction of lymph node metastasis in colorectal cancer: a systematic review and meta-analysis. Int J Surg. 2024 Jun 1;110(6):3795-3813. doi: 10.1097/JS9.0000000000001239.

[8]Nicastri DG, Doucette JT, Godfrey TE, Hughes SJ. Is occult lymph node disease in colorectal cancer patients clinically significant? A review of the relevant literature. J Mol Diagn. 2007 Nov;9(5):563-71. doi: 10.2353/jmoldx.2007.070032. Epub 2007 Oct 4. PMID: 17916603; PMCID: PMC2049052.

[9]Filipe EC, Chitty JL, Cox TR. Charting the unexplored extracellular matrix in cancer. Int J Exp Pathol. 2018 Apr;99(2):58-76. doi: 10.1111/iep.12269.

[10]Rigoglio NN, Rabelo ACS, Borghesi J, de Sá Schiavo Matias G, Fratini P, Prazeres PHDM, Pimentel CMMM, Birbrair A, Miglino MA. The Tumor Microenvironment: Focus on Extracellular Matrix. Adv Exp Med Biol. 2020;1245:1-38. doi: 10.1007/978-3-030-40146-7_1.

[11]Zhang Y, Wen Y, Li S, Deng L, Han T, Jing M, Zhao J, Zhou J. Combination of single-source dual-energy computed tomography (CT) parameters and extracellular volume fraction for predicting lymphovascular and perineural invasion in colorectal cancer. Quant Imaging Med Surg. 2024 Oct 1;14(10):7524-7539. doi: 10.21037/qims-24-76.

[12]Li J, Zou L, Ma H, Zhao J, Wang C, Li J, Hu G, Yang H, Wang B, Xu D, Xia Y, Jiang Y, Jiang X, Li N. Interpretable machine learning based on CT-derived extracellular volume fraction to predict pathological grading of hepatocellular carcinoma. Abdom Radiol (NY). 2024 Oct;49(10):3383-3396. doi: 10.1007/s00261-024-04313-9.

[13]Ming S, Zhang W, Wang M, Li J, Shi D, Wang B, Li M, Zhang Y, Zhu C, Sun A, Wei W. Contrast-enhanced CT-Derived extracellular volume fraction predicts survival in postoperative pancreatic cancer patients. Eur J Radiol. 2025 Oct;191:112273. doi: 10.1016/j.ejrad.2025.112273.

[14]Wang ZH, Song ZQ, Guo R, et al. Prediction of Ki-67 expression in hepatocellular carcinoma with a computed tomography (CT) extracellular volume-derived nomogram. Clin Radiol. 2025;88:106989. doi:10.1016/j.crad.2025.106989

[15]Ming S, Zhang W, Wang M, Li J, Shi D, Wang B, Li M, Zhang Y, Zhu C, Sun A, Wei W. Contrast-enhanced CT-Derived extracellular volume fraction predicts survival in postoperative pancreatic cancer patients. Eur J Radiol. 2025 Oct;191:112273. doi: 10.1016/j.ejrad.2025.112273.

[16]Guan Z, Wang ZH, Zhang XY, Yan S, Xu T, Li J, Shen L, Sun YS. Predicting Regional Lymph Node Metastases at CT in Microsatellite

Instability-High Colon Cancer. Radiology. 2025 Apr;315(1):e242122. doi: 10.1148/radiol.242122.

[17]Li Q, Hong R, Zhang P, Hou L, Bao H, Bai L, Zhao J. A clinical-radiomics nomogram based on spectral CT multi-parameter images for preoperative prediction of lymph node metastasis in colorectal cancer. Clin Exp Metastasis. 2024 Oct;41(5):639-653. doi: 10.1007/s10585-024-10293-3.

[18]Hong EK, Landolfi F, Castagnoli F, Park SJ, Boot J, Van den Berg J, Lee JM, Beets-Tan R. CT for lymph node staging of Colon cancer: not only size but also location and number of lymph node count. Abdom Radiol (NY). 2021 Sep;46(9):4096-4105. doi: 10.1007/s00261-021-03057-0.

[19]Yin J, Zhu W, Feng S, Yan P, Qin S. The role of cancer-associated fibroblasts in the invasion and metastasis of colorectal cancer. Front Cell Dev Biol. 2024;12:1375543. Published 2024 Jul 30. doi:10.3389/fcell.2024.1375543.

[20]Miyashita N, Saito A. Organ Specificity and Heterogeneity of Cancer-Associated Fibroblasts in Colorectal Cancer. Int J Mol Sci. 2021 Oct 11;22(20):10973. doi: 10.3390/ijms222010973.

[21]Wang W, Fan X, Yang J, Wang X, Gu Y, Chen M, Jiang Y, Liu L, Zhang M. Preliminary MRI Study of Extracellular Volume Fraction for Identification of Lymphovascular Space Invasion of Cervical

Cancer. J Magn Reson Imaging. 2023 Feb;57(2):587-597. doi: 10.1002/jmri.28423.

[22]Bian X, Xiao YT, Wu T, Yao M, Du L, Ren S, Wang J. Microvesicles and chemokines in tumor microenvironment: mediators of intercellular communications in tumor progression. Mol Cancer. 2019 Mar 30;18(1):50. doi: 10.1186/s12943-019-0973-7.

[23]Yang C, Cao F, Huang S, Zheng Y. Follistatin-Like 3 Correlates With Lymph Node Metastasis and Serves as a Biomarker of Extracellular Matrix Remodeling in Colorectal Cancer. Front Immunol. 2021 Jul 16;12:717505. doi: 10.3389/fimmu.2021.717505.

Supplementary Files

This is a list of supplementary files associated with this preprint. Click to download.

- Supplementarymaterail.docx